Final Draft
of the original manuscript:

Molcan, M.; Petrenko, V.I.; Avdeev, M.V.; Ivankov, O.I.; Haramus, V.M.; Skumiel, A.; Josefczak, A.; Kubovcikova, M.; Kopcansky, P.; Timko, M.:

Structure characterization of the magnetosome solutions for hyperthermia study

In: Journal of Molecular Liquids (2016) Elsevier

DOI: 10.1016/j.molliq.2016.12.054

Structure characterization of the magnetosome solutions for hyperthermia study

M. Molcan[1], V.I.Petrenko[2, 3], M.V. Avdeev[2], O.I. Ivankov[2], V.M. Garamus[4], A. Skumiel[5], A. Jozefczak[5], M. Kubovcikova[1], P. Kopcansky[1], M. Timko[1]

[1]Institute of Experimental Physics Slovak Academy of Sciences, Košice, Slovakia
[2]Joint Institute for Nuclear Research, 141980, Dubna, Russia
[3]Taras Shevchenko National University of Kyiv, Kyiv, Ukraine
[4]Helmholtz-Zentrum Geesthacht: Centre for Materials and Coastal Research, Max-Planck-Street 1, 21502 Geesthacht, Germany
[5]Institute of Acoustics, Faculty of Physics, Adam Mickiewicz University, Poznan, Poland

Abstract

Structure characterization of the initial magnetosome chain solution (IM) and mechanically treated magnetosome solution (SM) was done by dynamic light scattering (DLS), small-angle neutron (SANS) and X-ray (SAXS) scattering. Experimental scattering curves of magnetosome IM and SM samples indicate the presence of polydisperse particles in the investigated solutions. Predominant amount of non-magnetic components (most probably lipids) was found from SANS contrast variation experiment. The values of forward scattering intensities confirm the differences in average sizes of samples prepared by various methods. The effect of sonication and filtering on size distribution and polydispersity was also confirmed by evaluating of hydrodynamic size distribution. This fact causes that SM sample magnetically behaves in a different manner showing that energy losses and specific absorption rate are noticeable reduced, and that indicates variation in the relaxation process and heat distribution.

1. Introduction

Magnetosomes are nanosized particle structures assembled into chains. They are synthesized in magnetotactic bacteria. From the magnetosome application point of view the big effort is to use them in the field of magnetic hyperthermia [1, 2, 3]. Although any "*in vivo*" hyperthermia experiments using magnetosome particles are known, this effort is justified. It is based on their "core-shell" structure. Magnetosome consists of the magnetic core (in most cases Fe_3O_4 crystal) and cover shell on the organic base (phospholipid layer and various specific proteins). The diameter of magnetite core is mostly at the level of 40 ± 10 nm and the thickness of lipid shell is around 3-4 nm [4, 5, 6]. Moreover the fact that they are formed in chains multiplies their sensitivity to the magnetic field. It is connected with the increase in magnetocrystalline anisotropy [7]. This fact is manifested mainly in hyperthermic parameter SAR (Specific Absorption Rate) defined as the amount of heat released by a unit weight of the material per time unit during exposure to an oscillating magnetic field of defined frequency and field strength [8]. The requested hyperthermic properties (which are narrowly connected with relaxation times during AC experiment) depend strongly on the morphology (size, shape) and the degree of polydispersity [1, 7, 9]. So the essential is to obtain magnetosomes with precisely tailored properties by controlling and tuning their morphology, size and shape distribution. The control of magnetosome parameters is generally performed by changing the cultivation conditions that have a direct effect on crystal growth [7, 10, 11]. But there is also a possibility to change the magnetosome parameters by mechanical way in sonication or ultracentrifugation process [12]. The control of these parameters allows better to predict the heat generation in magnetosome samples during real hyperthermia experiment.

Selecting an appropriate investigation method is of great importance for the samples naturally occurring or prepared as solution. Many of available characterization methods, such

as electron microscopy give a lot of interesting information in the form of images, analysis of the composition or size distribution. The disadvantage is the requirement of dried or frozen samples while the sample properties are dramatically changed. Therefore, it has a great sense to carry out the characterization of these systems in the conditions, which do not affect the sample properties - i.e. that in the case of the solution of nanoparticles to investigate them in real current conditions and not in the form of dried or frozen state. Such methods are, for example, small-angle scattering techniques, magnetization measurements and dynamic light scattering [9, 13]. Recently small-angle scattering techniques were successfully used for structural investigation of various magnetic fluids type [14, 15, 16] and also for solutions of magnetic nanoparticles inside protein shell [17, 18]. The aim of the given work was to perform structure characterization of various magnetosome solutions and to compare its structure parameters with magnetic and hyperthermia results. Structure characterization of the various magnetosome solutions was done by dynamic light scattering (DLS), small-angle neutron (SANS) and X-ray (SAXS) scattering.

2. Material and methods

2.1 Magnetosome synthesis, isolation and purification

Bacterial magnetosomes were synthesized by the biomineralization process of magnetotactic bacteria Magnetospirillum strain AMB-1. Bacteria produce magnetite - Fe_3O_4 particles. Magnetospirillum Magnetotacticum sp. AMB-1 was grown microaerobically at 25°C in growth medium for a period of two weeks. The isolation process of magnetosome chains from the body of bacteria consists of a series of sonication cycles (in the ultrasonic bath), centrifugation and magnetic decantation. The supernatant was pipetted away and the sediment of magnetosome chains in the container was diluted with buffer 20 mM 4-(2-hydroxyethyl) -1- piperazineethanesulfonic acid (HEPES) + 4 mM ethylenediaminetetraacetic acid (EDTA): first 2 cycles, followed by washing with 10 mM HEPES - NaCl (3^{rd} cycle) and finally washing the samples with 10 mM HEPES (about 10 cycles times in order to make the most perfect purification of the sample). The buffers were adjusted to pH 7.4 by using KOH. These procedures leave the surrounding membrane intact and magnetosome preparations are apparently free of contaminating material. Owing to the presence of the enveloping membrane, isolated magnetosome particles form stable and well-dispersed suspensions.

2.2 Modification of magnetosome parameters

Sonication process

The isolated magnetosome chains were dispersed in HEPES buffer and divided in half. The first half represented isolated magnetosome chains (*sample IM*), which have not been modified additionally. The second half of the sample was exposed to the effects of sonifier cell disrupter by BRANSON (model 450), in order to obtain the individual magnetosomes by cutting of magnetosome chains (*sample SM*).

Microtip probe of the sonifier was immersed into the solution of isolated magnetosome chains dispersed in 10 mM HEPES buffer having a pH 7.4. The sample was sonicated at the power of 200 W for 3 hours in continuous mode at 20 kHz mechanical vibration. The ultrasonic tank was continuously cooled down by ice added to the bath to prevent thermal degradation of the sample. Sonication parameters were chosen in order to avoid damage or hard deformation of the biomembrane of magnetosomes as the material should keep their biocompatible character.

Filtration method

The reason for filtering arises from the effort of the elimination of large objects in the sample, obtaining the system with narrow size distribution and getting the individual magnetosome respectively magnetosome chains with a minimum number of particles bonded in the chain. IM and SM sample were filtered through the syringe membrane filters (*sample SM-F*). The pore sizes were 450 nm and 220 nm.

2.3. Evaluation methods for prepared magnetosome samples

SANS

SANS measurements were carried out on small-angle neutron scattering spectrometer YuMO at the pulsed nuclear reactor IBR-2 at the Joint Institute for Nuclear Research (JINR, Russia). Samples were located in standard quartz cuvettes (Hellma) with a thickness of 1 mm and the measurements were performed at room temperature. Neutron wavelengths range 0.05-0.8 nm was used. Measurement time per one sample was about 1 hour. The measured scattering curves were corrected for the scattering from the solvent and the absolute cross section was determined by vanadium calibration standards.

SAXS

The SAXS measurements were performed with a laboratory instrument (Nanostar, Bruker AXS GmbH, Karlsruhe, Germany) using the wavelength of the Cu Kα line. The accessible q range was 0.09 to 2.3 nm^{-1}. Samples were filled into glass capillaries of 2 mm diameter. The raw scattering data were corrected for the background from the solvent, black current of detector and shadow scattering of beamstop and converted to absolute units using the scattering of pure water measured at 20°C (program SuperSAXS, Prof. C. L. P. de Oliveira and Prof. J. S. Pedersen).

DLS

Dynamic light scattering was used for characterization of hydrodynamic size distribution of magnetosome particles dispersed in a liquid medium. The size of particles is calculated from the translational diffusion coefficient related to the velocity of Brownian motion by using the Stokes-Einstein equation. The measurements were carried out using Malvern Zetasizer Nano ZS (Malvern, UK). A small amount of magnetosomes suspension (~20 μl) was diluted with 1 ml of HEPES and measured in a disposal cell at 173° scattering angle, 25°C.

Magnetization measurements

Magnetization measurements of the prepared magnetosomes suspension were carried out by QD MPMS SQUID XL7 magnetometer at room temperature up to field intensity 1000 Oe.

AC calorimetry

Calorimetric investigations were performed in the testing system produced at IEP, Kosice. The alternating magnetic field was generated in the middle of the solenoid. Into the cavity of coil magnetosome sample was placed in glass vial (1 ml) and into this glass vial was immersed FISO FPI-HR thermometer, equipped with the FOT-L-BA optical sensor for temperature recording in time at given frequency and applied magnetic field. The accuracy of temperature measurements is 0.01K. The stable starting temperature was held by water flow through the plastic tube under winding. The high-frequency sinusoidal signal was amplified by the power amplifier, model AL-600-HF-A, which was connected to the LC circuit. By adjusting capacity it was possible to tune the system to the resonance frequency.

3. Results and discussion

Size distribution of magnetosomes investigated by DLS and small-angle scattering techniques

Figure 1 shows the intensity of normalized size distribution for initial (unfiltered) IM (a) and SM (b) magnetosome samples and also solutions which were additionally filtered through the syringe filters.

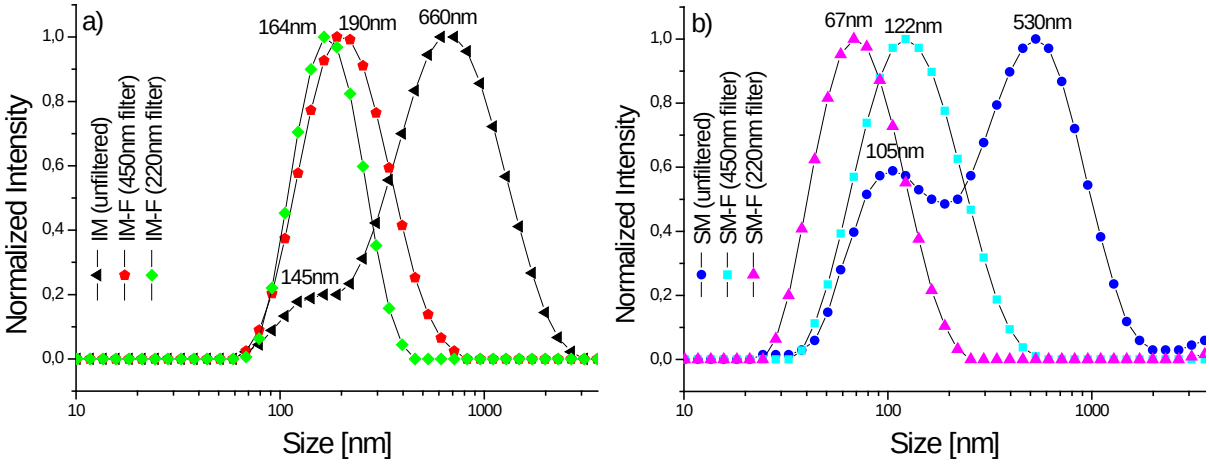

Fig. 1 DLS measurement: normalized intensity size distribution of magnetosomes. Curves represent IM and SM liquid samples, respectively. IM and SM samples which were filtered through the syringe filters with pore size of 450 nm and 220 nm (IM-F, SM-F).

IM sample exhibits a broader size distribution in comparison to SM sample. One can also see that the peak of the hydrodynamic size distribution is shifted towards smaller values (530 nm) for SM sample as compared to IM sample (660 nm). Unfiltered samples exhibited bimodal size distribution (minor population peaks at 145 nm and 105 nm for IM and SM, respectively were also observed). Filtering through the 450 nm and 220 nm pore size caused a significant drop in the size distribution in both types of samples. In the case of unfiltered IM sample with the major peak of the hydrodynamic size distribution at the level 660 nm, this value decreased to 164 nm and in the case of SM sample this value was shifted from 530 nm (major peak) to 67 nm, when 220 nm filter was used. The process of sonication and filtration has the evident impact on the hydrodynamic size distribution of magnetosome chains. These methods are promising tools for tuning size distribution of magnetosome chains.

As a key methodology, which can be considered as non-invasive and non-destructive we used the SANS and SAXS. Experimental SANS curves for classically prepared magnetosomes (not sonicated) - IM and sonicated magnetosomes - SM and SM-F (220 nm) samples are presented on fig. 3. The concentration of the magnetite in all samples was ≈ 0.16 mg/ml (estimated by UV/VIS spectrophotometric method).

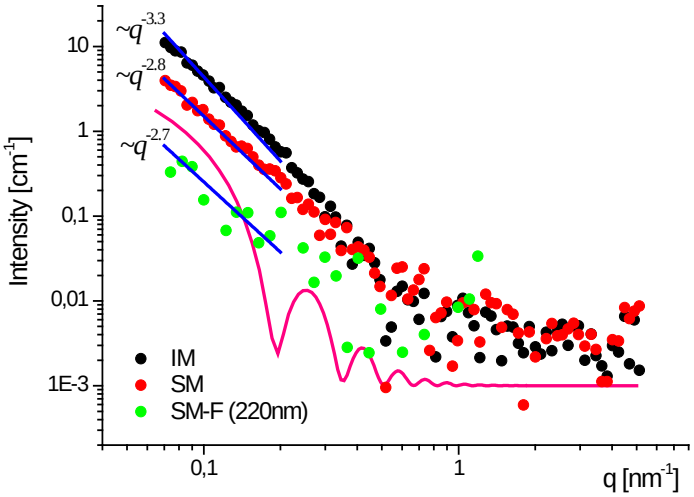

Fig. 2 Experimental SANS curves of IM, SM and SM-F (220 nm) magnetosome samples dissolved in HEPES buffer. Blue lines represent power law fit and pink – model curve for cylinder-like objects.

As it is seen from fig. 2 on the SANS curves there are no any specific oscillations and some power law at small q values is observed for all samples. Because magnetosomes are formed in chain-line structures we have tried to describe the scattering curves by the form-factor for elongated objects: cylinder model for a single chain (pink line at fig. 2). It should be mentioned that model of long big cylinder does not fit experimental SANS data. This indicates, that in our investigated sample we do not have individual singe chains, but they probably aggregate and create bigger objects with complicated composition. Thus quite big and polydisperse objects are presented in the investigated samples. Values of power law exponents are different for IM and SM samples and correspond to fractal aggregates. The initial parts of scattering curves of IM, SM and SM-F (220 nm) samples were fitted by "power-law" model (blue lines): $I(q)=Aq^{p}Aq^{-p}$, where A is a constant proportional to the neutron contrast and concentration, p is the power law exponent [19]. The values of the power-law exponent are 3.3, 2.8, and 2.7 for IM, SM and SM-F (220nm) sample correspondingly. We could say that sonication treatment transfers observed aggregates from the surface to mass fractals. The values of initial scattering intensities confirm the differences in average sizes in both kinds of samples. It is known that forward scattering intensity $I(0)$, is proportional to particles concentration, c; square of the contrast (difference between scattering length density of the buffer and particle), $\Delta\rho$; and square of the particles volume, V. If we assume that concentration and contrast are the same for IM and SM samples, then intensity ratio in small q values is proportional to square of the particles volumes ratio:

$$\frac{V_{IM}}{V_{SM}} = \sqrt{\frac{I_{IM\ (at\ q_{min})}}{I_{SM\ (at\ q_{min})}}} = \sqrt{\frac{11.05}{3.93}} = 1.68\,,(q_{min} = 0.007).$$

Based on this we can estimate that after sonication the mean volume of the scattering object was reduced ≈ 1.68 times. Since the volume is proportional to the radius in power 3 ($V \sim R^3$) we can also estimate radius ratio from DLS hydrodynamic diameter data for IM and SM (660 nm and 530 nm correspondingly). The volume ratio calculated from DLS ≈ 1.9 is in good agreement with the value obtained from SANS. Therefore we can conclude that sonication process really provides the remarkable effect on shortening of magnetosome chains/scattered objects size.

SANS signal from SM-F (220 nm) sample decreases because of concentration dropped at the value 0.08 mg/ml after filtration. The concentration decrease causes very bad statistic, but anyway the character of the curve is very similar to SM.

Volume fractions of magnetite and non-magnetite (lipids) components can be derived from the contrast variation experiment. SANS curves for IM and SM magnetosome suspensions (presented on fig. 3a and 3b) were measured at the 0%, 15%, 30% and 50% of D_2O content in solutions.

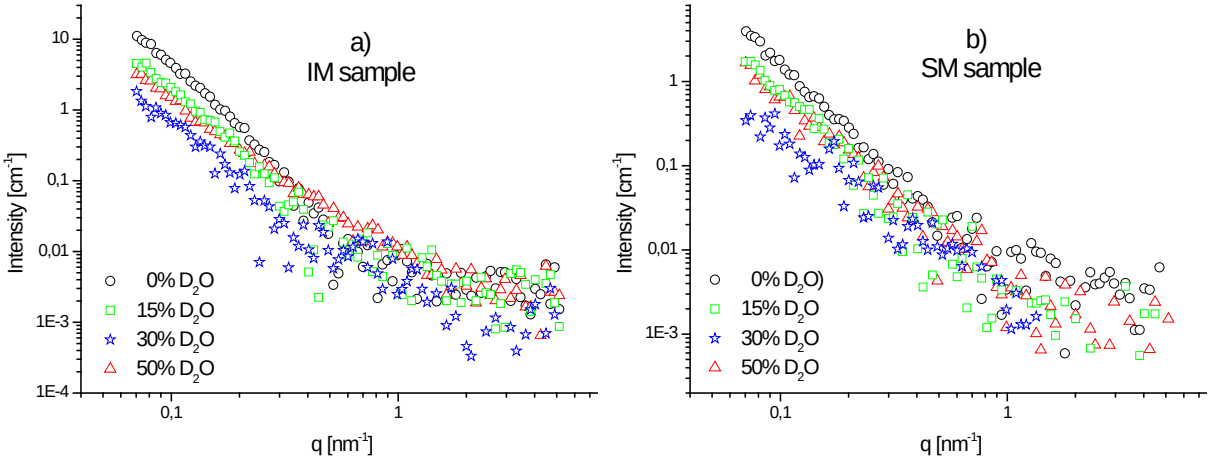

Fig. 3 SANS curves of IM and SM magnetosome solution in various ratios of H_2O and D_2O

Scattering intensities at low q ($q \approx 0.01$) were estimated from the experimental SANS curves at fig. 3 and dependence of the scattering intensity at low q vs. fraction of D_2O in the solvent were plotted and fitted by the parabola (fig. 4).

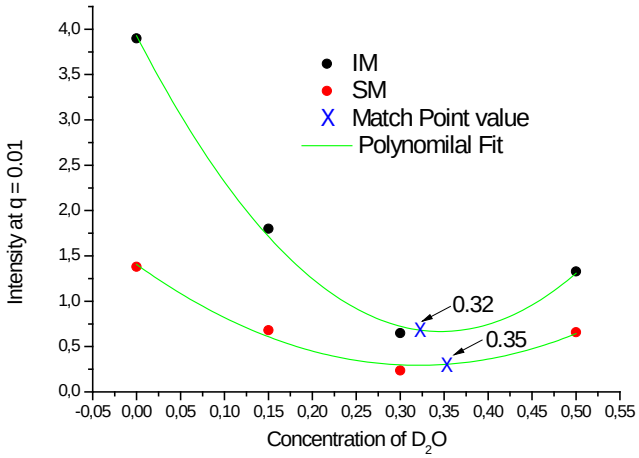

Fig. 4 Scattering intensity at the low angle (q= 0.01) as a function of the D_2O content. The minima of the fitted parabolas show the effective match points.

The scattering length densities (SLDs) of the particles (density in the match point $\rho_{solvent} = \rho_{Particle}$) $\bar{\rho}_{S_{IM}} = 1.64 * 10^{10} cm^{-2}$ and $\bar{\rho}_{S_{SM}} = 1.85 * 10^{10} cm^{-2}$ were calculated according to:

$$\bar{\rho}_S = x_{D_2O} * \rho_{D_2O} + (1 - x_{D_2O}) * \rho_{H_2O},$$

where $\rho_{H_2O} = -0.56 * 10^{10}\, cm^{-2}$ and $\rho_{D_2O} = 6.34 * 10^{10} cm^{-2}$ are SLD of H_2O and D_2O, x_{D_2O} = 0.32 and 0.35 for IM and SM samples corresponds to the lowest value of I (0.01) named as ~~a~~ match point. Volume fraction ε of magnetite was calculated according to assumption that in magnetosome there are just two components, magnetite core with SLD $\rho_{Fe_3O_4} = 6.9 * 10^{10}\, cm^{-2}$ and protein shell, $\rho_{shell} = 0.48 * 10^{10}\, cm^{-2}$:

$$\varepsilon = \frac{\bar{\rho} - \rho_{shell}}{\rho_{Fe_3O_4} - \rho_{shell}}.$$

Thus according to the obtained $\bar{\rho}_{S_{IM}}$ and $\bar{\rho}_{S_{SM}}$, the volume fraction of magnetite were estimated as ≈ 18% and 21% for IM and SM, respectively. These values are very low if we introduce magnetosomes as big magnetite core which is surrounded by a thin protein shell. From the TEM images presented in our previous papers [4, 12] we know that one magnetosome particle has approx. spherical shape with 40 nm big size core and 2-3 nm thick shell. On behalf of these facts we expected values at the level around 80% of Fe_3O_4. We repeated this experiment again with new prepared magnetosomes for 0%, 25%, 50%, 75% and 100% of D_2O content and the results were approximately the same similar: 32% and 26% for volume fraction of Fe_3O_4, for IM and SM, respectively (data are not shown). This finding confirms that magnetosome chains create complex objects where organic bacterial components (lipids and trapped organic stuffs) are major in the sample.

It should be mentioned that some dark precipitates were observed for all solutions. These precipitates were easily re-dissolved/ re-dispergented by ultrasound stirring. Nevertheless from supernatant we have got quite good SAXS signal with sufficient intensity. It means that in the volume are still present the nanoscopic magnetosome parts. Unlike previous SANS case (fig. 3) where signal just from large aggregates was observed, in supernatant by SAXS (fig. 5) only from smaller size could be seen (saturation of the scattering signal at smallest *q*-values). From the obtained SAXS curves pair distance distribution function of magnetite core was calculated since the X-ray scattering contrast of magnetite is almost 100 higher than for lipid part. The analysis of the scattering data has been done applying the Indirect Fourier Transformation method (IFT) developed by O. Glatter [20] in the version of J. S. Pedersen [21]. This model independent approach needs only minor additional (model) information on the possible aggregate structure: dimensions (sphere-like, rod-like or disc-like) and the maximal value of the diameter, cross section diameter or thickness, respectively.

In the present study, the values of D_{max} were carefully chosen to give both good fits to the experimental data and smooth *p(r)* functions.

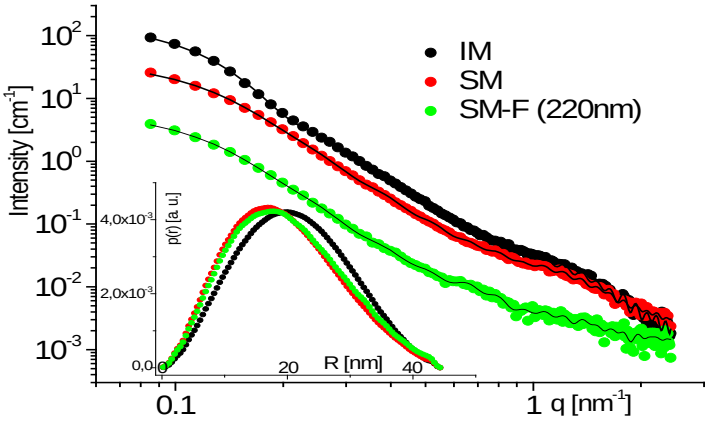

Fig 5 Experimental SAXS curves for IM, SM and SM-F (220nm) samples. Inset represents the pair distance distribution of magnetosome cores.

The position maximum at *p(r)* function and obtained radius of gyration is decreased for SM and SM-F samples (~ 17 nm and 15 nm) to compare with IM (~ 20 nm and 16 nm). This fact gives us the information, that during sonication the organic shell was not disrupted because the size distribution increases due to agglomeration of non-covered particles.

Radius of gyration of the scattering objects was calculated from the initial part of SAXS curves.

Magnetic properties of magnetosome IM and SM suspension

The effect of sonication on magnetic properties of magnetosome suspensions is showed on fig. 6. The hysteresis loops measured at temperature 293 K show a ferromagnetic behavior of magnetosome samples with the same saturation magnetization M_S = 1.7 emu.g^{-1} and coercive field 16 Oe, and 7 Oe for IM and SM, respectively.

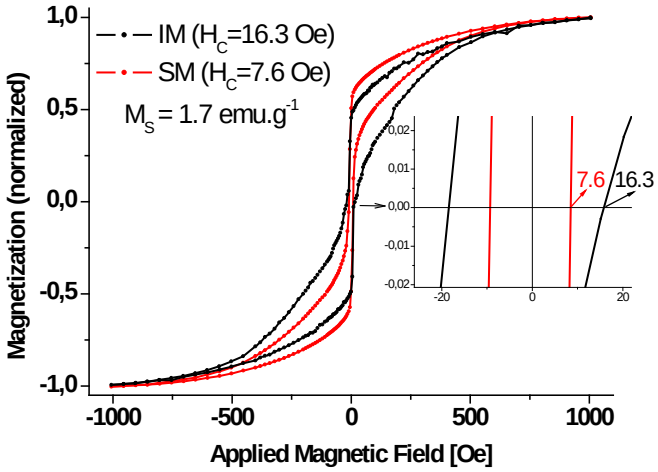

Fig. 6 Hysteresis loops for sample IM and SM.

The orderly arranged magnetosomes in the chains have strong interparticle dipolar interactions, so exhibiting a higher coercivity than separate magnetite nanoparticles. It is the main reason why in sonicated sample containing partly individual particles the coercive force is lower as for isolated sample.

On the other hand, hysteresis loop of presented samples have unusual wasp-waisted shape that is constricted in the middle. The wasp-waisted shape is thought to arise from the fact that the grains dispersed have a distribution of sizes and so coercive fields too. The wasp-waisted hysteresis loop is a superposition of two *M–H* loops with different coercivity. It is observed for the materials that contain two different types of magnetic orderings simultaneously or a very large size distribution of particles [22]. The size distribution of our samples (DLS experiment – see fig. 1) shows two peaks in distribution what can be the ~~as a~~ reason for this type of hysteresis loop in used magnetosome solution before and after sonication effect.

Impact of magnetosome chains parameters on hyperthermia results

Time dependences of temperature for IM and SM sample were measured at the various magnetic field intensities H (up to 2.7 kA.m^{-1}) and at the constant frequency f = 508 kHz (fig. 7).

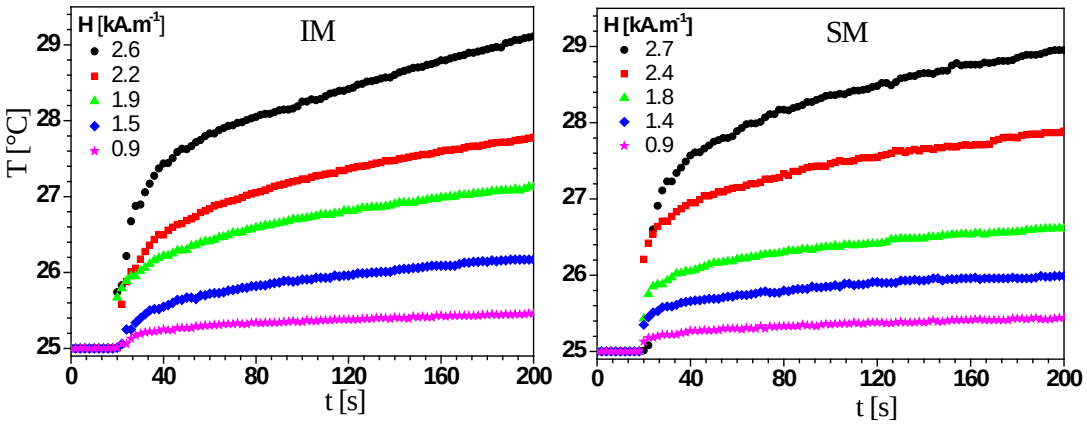

Fig. 7 Time evolution of temperature of IM and SM magnetosome samples during the exposition to various AC magnetic field intensities *H* at the frequency *f* = 508 kHz.

As the applied magnetic field *H* increased the heating rate *ΔT/Δt* dynamically increased too [results for the same kind of samples are also presented in 17]. The *ΔT/Δt* values were estimated at each applied field by the linear fit of *T* vs *t* experimental data in the range 25-35 seconds. The *ΔT/Δt* as a function of applied magnetic field dependencies for IM and SM were fitted by the function $\Delta T/\Delta t = (H/a)^n$. According to [23, 24] it is known that *ΔT/Δt* is proportional to H^2 in the case of relaxation processes and to H^3 in the case of hysteresis processes. Because the fitting parameter *n* exceeds 2 in both cases (IM, SM) we have to take into account both mechanisms – relaxation and hysteresis. In general for $2 \leq n \leq 3$ the presence of superpara- and ferrimagnetic particles is expected. Due to the existence of shorter chains and even individual magnetosomes nanoparticles for SM sample the number of superparamagnetic parts in the sample volume increases and thus the energy contribution coming from the hysteresis processes (ferrimagnetic particles) contributes less. It is attributed to a higher rotational freedom of shortened magnetosomes. The *SAR* values relative to 1 gram of the sample extrapolated to the field strength *H* = 10 kA·m^{-1} are presented in the table 1.

Tab. 1 Fitting parameters *a*, *n* and *ΔT/Δt*, *SAR* values extrapolated to 10 kA.m^{-1} for IM and SM samples determined on the basis of the calorimetric experiment.

Sample	a	n	$\Delta T/\Delta t$	$SAR = C_P \cdot \left(\frac{\Delta T}{\Delta t}\right)$
	$\left[A \cdot m^{-1} \cdot s^{\frac{1}{n}} \cdot K^{-\frac{1}{n}}\right]$	-	[K·s^{-1}]	$\left[mW.g_{sample}^{-1}\right]$
IM	20131	2.27	0.189	934
SM	27617	2.21	0.106	486

The SAR reducing from 934 mW/g for IM to 486 mW/g for SM really indicates the big impact of sonication on magnetosome properties (chains sizes – number of magnetosomes per chain, magnetic properties - coercivity) and thus on the relaxation process and heat distribution of the variously treated samples.

4. Conclusion

Building on our previous experiments we opened the new possibilities for characterization of magnetosomes using neutron and X-ray scattering techniques. Using

SANS measurements the volume fraction of magnetosome parts (magnetite and lipids) diluted in liquid carrier was calculated. It was found that in the sample volume is high amount of light components which are probably trapped in the magnetosome chain structures. From SAXS measurements we were able to calculate pair distance distribution function of magnetite core. The diameter of magnetite cores was estimated to be 40 nm. Both techniques also confirmed the consequences of changes in methodology of magnetosome IM and SM samples preparation. The mean volume of the scattering object was reduced ≈ 1.68 times after sonication. The volume ratio calculated from DLS ≈ 1.9 and it is in good agreement with the value obtained from SANS. Based on this we can conclude that the sonication process really provides the remarkable effect on shortening of magnetosome chains/scattered objects size. The effect of sonication was resulted in magnetic and hyperthermia results. The hysteresis loops of measured magnetosome solution have unusual wasp-waisted shape arising from fact that the dispersed magnetic grains have a large distribution of sizes (longer and shorter chains and individual particles too) and also the coercive fields ~~too~~. According to this fact this type of hysteresis loop is a consequence of superposition of hysteresis loops with various coercivity. The SAR dropped from 934 mW/g for IM to 486 mW/g in the case of SM. The possibility of changing/controlling of magnetosome chain lengths may result in preparation of such systems in which we can better predict the heating parameters and distributions during hyperthermic experiments.

Acknowledgments

This work was supported by Slovak Scientific Grant Agency VEGA (projects no.00141 and 0045), by the European Structural Funds PROMATECH no. 26220220186, PHYSNET no.26110230097, M-ERA. NET MACOSYS and COST Radiomag TD1402 and Grant No. DEC-2015/17/B/ST7/03566 of the Polish National Science Centre and European Social Fund POKL.04.03.00-00-015/12),

References

[1] Alphandéry E, Guyot F Chebbi I, Preparation of chains of magnetosomes, isolated from Magnetospirillum magneticum strain AMB-1 magnetotactic bacteria, yielding efficient treatment of tumors using magnetic hyperthermia, International Journal of Pharmaceutics, Volume 434, Issues 1–2, 15 September 2012, pp. 444-452, ISSN 0378-5173

[2] Hergt R, Dutz S, Magnetic particle hyperthermia—biophysical limitations of a visionary tumour therapy, Journal of Magnetism and Magnetic Materials, Volume 311, Issue 1, April 2007, pp. 187-192, ISSN 0304-8853

[3] Timko M, Dzarova A, Kovac J, Skumiel A, Józefczak A, Hornowski T, Gojżewski H, Zavisova V, Koneracka M, Sprincova A, Strbak O, Kopcansky P, Tomasovicova N, Magnetic properties and heating effect in bacterial magnetic nanoparticles, Journal of Magnetism and Magnetic Materials, Volume 321, Issue 10, May 2009, pp. 1521-1524, ISSN 0304-8853

[4] Gojzewski H, Makowski M, Hashim A, Kopcansky P, Tomori Z, Timko M, (2012) 578 Magnetosomes on surface: An imaging study approach. Scanning 34: 159-169. 579

[5] Bazylinski DA, Schübbe S, Controlled Biomineralization by and Applications of Magnetotactic Bacteria, Advances in Applied Microbiology, Academic Press, 2007, Volume 62, Pages 21-62, ISSN 0065-2164, ISBN 9780123736697

[6] Ionescu A, Darton NJ, Vyas K, Llandro J, Detection of endogenous magnetic nanoparticles with a tunnelling magneto resistance sensor, Phil. Trans. R. Soc. A, 2010, 368, 4371-4387, doi:10.1098/rsta.2010.0137

[7] Timko M, Molcan M, Hashim A, Skumiel A, Müller M, Gojzewski H, Józefczak A, Kovac J, Rajnak M, Makowski M, Kopčanský P, Hyperthermic Effect in Suspension of Magnetosomes Prepared by Various Methods, IEEE Transactions on Magnetics, vol. 49, no. 1, pp. 250-254, Jan. 2013, doi: 10.1109/TMAG.2012.2224098

[8] Ramanujan RV, Lao LL, Magnetic Particles for Hyperthermia Treatment of Cancer, In: Proceeding, First International Conference on Bioengineering and Nanotechnology September 26 - 29, 2004, Bipolis, Singapore

[9] Schwamberger A, De Roo B, Jacob D, Dillemans L, Bruegemann L, Seo JW, Locquet JP, Combining SAXS and DLS for simultaneous measurements and time-resolved monitoring of nanoparticle synthesis, Nuclear Instruments and Methods in Physics Research Section B: Beam Interactions with Materials and Atoms, Volume 343, 15 January 2015, Pages 116-122, ISSN 0168-583X

[10] Hashim A, Molčan M, Kováč J, Varchulová Z, Gojzewski H, Makowski M, Kopčanský P, Tomori Z, Timko M, The Influence of Morphology on Magnetic Properties of Magnetosomes, Acta Physica Polonica A, Vol. 121 (2012) No. 5 6, s. 1250 – 1252

[11] Silva KT, Leão PE, Abreu F, López JA, Gutarra ML, Farina M, Bazylinski DA, Freire DMG, Lins U, Optimization of magnetosome production and growth by the magnetotactic vibrio Magnetovibrio blakemorei strain MV-1 through a statistics-based experimental design. Appl. Environ. Microbiol. 2013, 79, 2823-2827.

[12] Molcan M, Hashim A, Kovac J, Rajnak M, Kopcansky P, Makowski M, Gojzewski H, Molokac M, Hvizdak L, Timko M, Characterization of Magnetosomes After Exposure to the Effect of the Sonication and Ultracentrifugation, 2014, Acta Phys. Pol. A, 126, 198–199, doi: 10.12693/APhysPolA.126.198.

[13] Svergun DI, Koch MHJ, Small angle scattering studies of biological macromolecules in solution Rep. Prog. Phys., 66 (2003), pp. 1735-1782

[14] Petrenko VI, Aksenov VL, Avdeev MV, Bulavin LA, Rosta L, Vekas L, Garamus VM, Willumeit R, Analysis of the structure of aqueous ferrofluids by the small-angle neutron scattering method. Physics of the Solid State 52(5) (2010) 974-978

[15] Petrenko VI, Avdeev MV, Garamus VM, Bulavin LA, Aksenov VL, Rosta L, Micelle formation in aqueous solutions of dodecylbenzene sulfonic acid studied by small-angle neutron scattering. Colloids Surf. A 369 (2010) 160-164

[16] Petrenko VI, Avdeev MV, Aksenov VL, Bulavin LA, Rosta L, Magnetic fluids with excess of a surfactant according to the data of small-angle neutron scattering, Journal of Surface Investigation. X-ray, Synchrotron and Neutron Techniques 3(1) (2009) 161-164

[17] Melníková L, Petrenko VI, Avdeev MV, Garamus VM, Almásy L, Ivankov OI, Bulavin LA, Mitróová Z, Kopčanský P, Effect of iron oxide loading on magnetoferritin structure in solution as revealed by SAXS and SANS, Colloids and Surfaces B: Biointerfaces, Vol. 123, 2014, 82-88, ISSN 0927-7765, http://dx.doi.org/10.1016/j.colsurfb.2014.08.032.

[18] L.Melnikova, V.I.Petrenko, M.V.Avdeev, O.I.Ivankov, L.A.Bulavin, V.M.Garamus, L.Almásy, Z.Mitroova, P.Kopcansky. SANS contrast variation study of magnetoferritin

structure at various iron loading. Journal of Magnetism and Magnetic Materials 377 (2015) 77–80

[19] Knott RB, Lin M, Hanley MJM, Muir D, Preliminary SANS studies of the structure of nickel powders on the nanoscale, Physica B: Condensed Matter, Vol. 385–386, Part 2, 2006, 908-910, ISSN 0921-4526, http://dx.doi.org/10.1016/j.physb.2006.05.246.

[20] Glatter O, A New Method for the Evaluation of Small-Angle Scattering Data, J. Appl. Crystalogr., 10, 1977, 415-421.

[21] Pedersen JS, Analysis of Small-Angle Scattering Data from Colloids and Polymer Solutions: Modeling and Least-squares Fitting Adv. Coll. Inter. Sci., 70, 1997, 171-210

[22] Yang Ch, Jiang JS, Wang ChM, Zhang WG, A unique magnetic behavior and dielectric properties of Bi0.9–xLa0.1CaxFeO3 nanoparticles at room temperature, Journal of Physics and Chemistry of Solids, Vol. 73, Issue 1, 2012, pp 115-119, ISSN 0022-3697, http://dx.doi.org/10.1016/j.jpcs.2011.10.021.

[23] Józefczak A, Leszczyński B, Skumiel A, Hornowski T, A comparison between acoustic properties and heat effects in biogenic (magnetosomes) and abiotic magnetite nanoparticle suspensions, Journal of Magnetism and Magnetic Materials, Vol. 407, 2016, pp 92-100, ISSN 0304-8853, http://dx.doi.org/10.1016/j.jmmm.2016.01.054.

[24] Skumiel A, Kaczmarek-Klinowska M, Timko M, et al. Int J Thermophys (2013) 34: 655. doi:10.1007/s10765-012-1380-0